Electron transport on a cylindrical surface with one-dimensional leads

V. A. Margulis and M. A. Pyataev*

Mordovian State University, Saransk, Russia

(Received 22 February 2005; revised manuscript received 24 May 2005; published 3 August 2005)

A nanodevice consisting of a conductive cylinder in an axial magnetic field with one-dimensional wires attached to its lateral surface is considered. An explicit form for transmission and reflection coefficients of the system as a function of electron energy is found from the first principles. The form and the position of transmission resonances and zeros are studied. It is found that, in the case of one wire being attached to the cylinder, reflection peaks occur at energies coinciding with the discrete part of the electronic spectrum of the cylinder. These peaks are split in a magnetic field. In the case of two wires the asymmetric Fano-type resonances are detected in the transmission between the wires for integer and half integer values of the magnetic flux. The collapse of the resonances appears for certain position of contacts. Magnetic field splits transmission peaks and leads to spin polarization of transmitted electrons.

I. INTRODUCTION

Electron transport in curved two-dimensional nanostructures attracts considerable attention in the last decade. Transport properties of the electron gas on spherical[1–5] and cylindrical[6,7] nanosurfaces have been intensively studied in the last few years. Those systems are of particular interest due to recent intensive experimental investigations of the coherent transport in individual carbon nanotubes[8–12] and rolled GaAs/AlGaAs heterostructures.[13,14] A number of theoretical works[15–22] have been focused on the electron transport in carbon nanotubes (see Ref. 23 for review). It should be mentioned that nanotube-based multiterminal nanodevices have recently attracted more and more attention since they are proposed as promising units for future low-power high-speed electronics. A lot of works[24–30] are devoted to the investigation of the electron transport in various interesting multiterminal nanodevices.

The conductance is usually measured for two basic geometries of contacts. Most theoretical studies are focused on the case of end-contacted nanotubes. In this geometry a strong interaction between metal and carbon atoms is realized, resulting in low contact resistance. However, in the last few years much attention has been devoted to side-contacted nanotubes.[31] In this case the leads are attached to the lateral surface of the tube. The interest to these structures is stipulated by recent experiments on scanned probe microscopy of electronic transport in the nanotubes.[32,33] The tip of the atomic force microscope can play the role of the side-contacted lead. Another interesting system with laterally attached leads is branched "nanotree" reported in Ref. 34. We mention that the side-contacted geometry is also realized in crossed carbon nanotubes.[9] It is evident that the lateral disposition of the contacts can significantly affect the transport. In particular, the resonant transport regime is expected in this case.

Recent experiments on the transport in carbon nanotubes[9,10] have reported the presence of asymmetric Fano resonances in the dependence of conductance on the Fermi energy. Being a characteristic manifestation of wave phenomena in scattering experiments, resonances have received considerable attention in recent electron transport investigations. A number of papers[35–38] are devoted to the study of Fano resonances in the transport through quasi-one-dimensional channels with impurities. It is shown in Refs. 4,5 that the same resonances occur in the conductance through a quantum nanosphere and a quantum nanotorus. Similar phenomena could be expected in the electron transport through the quantum cylinder but our analysis shows that the form of resonances differs from the Fano line shape.

The purpose of the present paper is an investigation of the electron transport through a multiterminal nanodevice consisting of a conductive cylindrical surface C with one-dimensional wires attached to it. The cylinder is placed in an axial magnetic field B and the wires are attached to its lateral surface. The number of wires we denote by N. We consider in detail the case of one and two wires attached to the cylinder. The points of contacts on the cylinder we denote by $\mathbf{q}_j = (z_j, \varphi_j)$, where z_j and φ_j are cylindrical coordinates and $j = 1, \ldots, N$ is the number of the contact.

In our model, the electron on the cylinder is able to go away from the contact region to infinity and never returns back. We stress that the model is valid for a realistic finite-size cylinder if its bases are immersed into absorbing electron reservoirs as shown in Fig. 1.

II. HAMILTONIAN AND TRANSMISSION COEFFICIENT

In the model, the wires are taken to be one dimensional and represented by semiaxes $\mathbb{R}_j^+ = \{x : x \geqslant 0\}$ ($j = 1 \cdots N$). They are connected to the cylinder by gluing the point $x = 0$ from $\mathbb{R}_j^+$ to the point $\mathbf{q}_j$ from C. We suppose $\mathbf{q}_i \neq \mathbf{q}_j$ for $i \neq j$. The scheme of the device is shown in Fig. 1.

If spin-orbital interaction is absent, then spin orientation conserves, and transmission coefficients $T^\uparrow(E)$ and $T^\downarrow(E)$ for electrons polarized in the direction of the magnetic field and in the opposite direction may be expressed in terms of the transmission coefficient $T(E)$ for spin-free scattering

$$T^\uparrow(E) = T(E - g\mu_B B/2), \quad T^\downarrow(E) = T(E + g\mu_B B/2),$$

where g is electron g-factor and μ_B is the Bohr magneton. Similar relations are valid for reflection coefficients. Further,
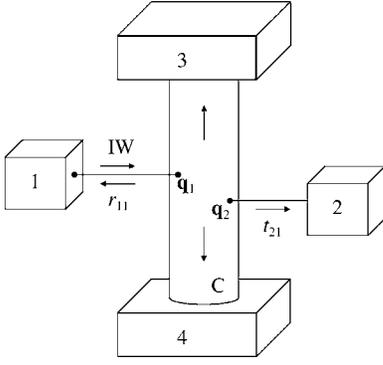
FIG. 1. Scheme of the device in the case of two wires attached to the cylinder. An incident wave (IW) originating from reservoir 1 is reflected back with amplitude r_{11} and scattered to reservoir 2 with amplitude t_{21}. Reservoirs 3 and 4 absorb the electron waves going away from the contact region.

we will deal with the spin-free problem and use spin indices only where it is necessary.

A wave function ψ of the electron in the device consists of $N+1$ parts:

$$\psi = \begin{pmatrix} \psi_C \\ \psi_1 \\ \cdots \\ \psi_N \end{pmatrix}, \qquad (1)$$

where ψ_C is a function on C and $\psi_j (j=1,\ldots,N)$ are functions on $\mathbb{R}_j^+$.

To obtain the Hamiltonian H of the whole system we use an approach based on the operator extension theory.[39,40] This method has been already used in Refs. 3–5 for the investigation of the electron transport through the nanosphere and the nanotorus.

The Hamiltonian H of the whole system is a point perturbation of the operator

$$H_0 = H_C \oplus H_1 \oplus \cdots \oplus H_N, \qquad (2)$$

where H_C is an electron Hamiltonian on the cylinder and H_j are Hamiltonians in the wires $\mathbb{R}_j^+$.

Using cylindrical coordinates, we can represent the Hamiltonian H_C in the form

$$H_C = \frac{p_z^2}{2m_c} + \frac{\hbar^2}{2m_c r^2}\left(i\frac{\partial}{\partial\varphi} - \frac{\Phi}{\Phi_0}\right)^2, \qquad (3)$$

where p_z is the z component of the momentum, r is the radius of the cylinder, m_c is the electron effective mass on the cylinder, $\Phi = \pi r^2 B$ is the magnetic flux, and $\Phi_0 = 2\pi\hbar c/|e|$ is the magnetic-flux quantum. It is convenient to represent the Hamiltonian H_C in the form $H_C = H_z + H_\varphi$ where $H_z = p_z^2/2m_c$ and $H_\varphi = (\hbar^2/2m_c r^2)[i(\partial/\partial\varphi) - \Phi/\Phi_0]^2$. We will need below the eigenvalues

$$E_m = \frac{\hbar^2}{2m_c r^2}\left(m + \frac{\Phi}{\Phi_0}\right)^2 \qquad (4)$$

and the eigenfunctions

$$\Psi_m(\varphi) = (2\pi r)^{-1/2}\exp(im\varphi) \qquad (5)$$

of the operator H_φ.

Electron motion in each wire $\mathbb{R}_j^+$ is described by the Hamiltonian $H_j = p_x^2/2m_w$, where p_x is the momentum operator and m_w is the effective mass for the electron in the wires.

To define the Hamiltonian H we use boundary conditions at points of gluing. The role of boundary values for the wave functions ψ_j is played, as usual, by $\psi_j(0)$ and $\psi_j'(0)$. The zero-range potential theory shows that to obtain a nontrivial Hamiltonian for the whole system we must consider functions ψ_C with a logarithmic singularity at the points of gluing $\mathbf{q}_j$,

$$\psi_C(\mathbf{x}) = -u_j\frac{m_c}{\pi\hbar^2}\ln\rho(\mathbf{x},\mathbf{q}_j) + v_j + o(1), \quad \text{as } \mathbf{x} \to \mathbf{q}_j. \quad (6)$$

Here u_j and v_j are complex coefficients and $\rho(\mathbf{x},\mathbf{q}_j)$ is the geodesic distance on the cylinder between the points $\mathbf{x}$ and $\mathbf{q}_j$. It is known that the most general self-adjoint boundary conditions are defined by some linear relations between $\psi_j(0)$, $\psi_j'(0)$, and the coefficients u_j and v_j. Following Ref. 4, we will write these conditions in the form

$$\begin{cases} v_j = \sum_{k=1}^{N}\left[B_{jk}u_k - \frac{\hbar^2}{2m_w}A_{jk}\psi_k'(0)\right], & j = 1\cdots N, \\[2mm] \psi_j(0) = \sum_{k=1}^{N}\left[A_{kj}^*u_k - \frac{\hbar^2}{2m_w}C_{jk}\psi_k'(0)\right]. \end{cases} \qquad (7)$$

Here complex parameters A_{jk}, B_{jk}, and C_{jk} are the elements of $N\times N$ matrices. The matrices B and C have to be Hermitian because the Hamiltonian H is a self-adjoint operator.[40] To avoid a nonlocal tunneling coupling between different contact points we will restrict ourselves to the case of diagonal matrices A, B, and C only. According to the zero-range potential theory diagonal elements of the matrix B determine the strength of point perturbations of the Hamiltonian H_C at the points $\mathbf{q}_j$ on the cylinder. These elements may be expressed in terms of scattering lengths λ_j^B on the corresponding point perturbations: $B_{jj} = m_c\ln(\lambda_j^B)/\pi\hbar^2$. Similarly elements C_{jj} describe the strength of point perturbations at the point $x=0$ in the wires and may be expressed in terms of scattering lengths λ_j^C by the relation $C_{jj} = -m_w\lambda_j^C/2\hbar^2$. For convenience, we represent parameters A_{jj} in the form $A_{jj} = m_w\sqrt{\lambda_j^A}e^{i\phi_j}/\hbar^2$, where λ_j^A has the dimension of length and ϕ_j is the argument of the complex number A_{jj}. We mention that the effect of the scattering lengths λ_j^A, λ_j^B, and λ_j^C on the electron transport has been discussed in Ref. 4. In the present paper we concentrate our attention on phenomena which are independent of contact parameters.

To obtain transmission and reflection coefficients of the system one needs a solution of the Schrödinger equation for the Hamiltonian H. The function ψ_1 in this solution is a superposition of incident and reflected waves while other functions $\psi_j (j=2,\ldots N)$ represent scattered waves. The wave function ψ_C may be expressed[4] in terms of the Green function $G(\mathbf{x},\mathbf{x}';E)$ for the Hamiltonian H_C,

$$\begin{cases} \psi_C(\mathbf{x}) = \sum_{j=1}^{N} \xi_j(E) G(\mathbf{x}, \mathbf{q}_j; E), \\ \psi_j(x) = \delta_{j1} e^{-ikx} + S_j(E) e^{ikx}, \quad j = 1, \ldots, N. \end{cases} \quad (8)$$

Here $k = \sqrt{2m_w E/\hbar^2}$ is the electron wave vector in wires, $\xi_j(E)$ are complex factors, and $S_j(E)$ is the amplitude of the outgoing wave in the wire $\mathbb{R}_j^+$.

It is well known that the Green function $G(\mathbf{x}, \mathbf{x}'; E)$ may be represented in the form

$$G(\mathbf{x}, \mathbf{x}'; E) = \sum_{m=-\infty}^{\infty} G_z(z, z'; E - E_m) \Psi_m(\varphi) \Psi_m^*(\varphi'), \quad (9)$$

where $\mathbf{x} = (z, \varphi)$, $\mathbf{x}' = (z', \varphi')$, and

$$G_z(z, z'; E) = \frac{im_c}{\hbar^2 k} e^{ik|z-z'|} \quad (10)$$

is the Green function of the operator H_z. Substituting Eq. (10) into Eq. (9), we get the following equation for $G(\mathbf{x}, \mathbf{x}'; E)$:

$$G(\mathbf{x}, \mathbf{x}'; E) = \frac{im_c}{2\pi\hbar^2} \sum_{m=-\infty}^{\infty} \frac{e^{ik_m|z-z'|+im(\varphi-\varphi')}}{k_m r}, \quad (11)$$

where $\hbar^2 k_m^2 = 2m_c(E - E_m)$, $\mathrm{Re}\, k_m > 0$ for $E > E_m$, and $\mathrm{Im}\, k_m > 0$ for $E < E_m$.

Considering the asymptotics (6) of $\psi_C(\mathbf{x})$ from Eq. (8) near the point $\mathbf{q}_j$, we have

$$u_j = \xi_j, \quad v_j = \sum_{i=1}^{N} Q_{ji}(E) \xi_i. \quad (12)$$

Here $Q_{ij}(E)$ is the Krein's Q-function, that is, $N \times N$ matrix with elements

$$Q_{ij} = \begin{cases} G(\mathbf{q}_i, \mathbf{q}_j; E), & i \neq j; \\ \lim_{\mathbf{x} \to \mathbf{q}_j} \left[G(\mathbf{q}_j, \mathbf{x}; E) + \frac{m_c}{\pi\hbar^2} \ln \rho(\mathbf{q}_j, \mathbf{x}) \right], & i = j. \end{cases}$$

Using the elementary relation

$$\sum_{n=1}^{\infty} \frac{\exp(-nx)}{n} = -\ln(1 - e^{-x}),$$

we can subtract the logarithmic singularity from $G(\mathbf{x}, \mathbf{x}'; E)$ and get the following form for diagonal elements of Q-matrix:

$$Q_{jj} = \frac{m_c}{2\pi\hbar^2} \left[\frac{i}{k_0 r} + \sum_{m=1}^{\infty} \left(\frac{i}{k_m r} + \frac{i}{k_{-m} r} - \frac{2}{m} \right) + 2 \ln r \right], \quad (13)$$

The similar method has been used in Ref. 41 for calculating the Q-function for electron Hamiltonian on a strip. It should be mentioned that Eq. (13) gives the Q-function for the free particle on a plane[42] in the case of $B = 0$ and $r \to \infty$.

Let us consider the asymptotics of $\psi_C(\mathbf{x})$ at $z \to \pm\infty$. As it follows from Eqs. (8) and (11), the wave function $\psi_C(\mathbf{x})$ is a superposition of propagating modes

$$\tilde{\Psi}_m^\pm(\varphi, z) = \Psi_m(\varphi) \exp(\pm ik_m z).$$

The highest and lowest numbers of the occupied modes we denote by $M^\pm = [\pm kr - \Phi/\Phi_0]$, where $[x]$ means the integer part of x. Using Eqs. (8) and (11), we obtain

$$\psi_C(\mathbf{x}) \simeq \sum_{m=M^-}^{M^+} t_m^\pm \tilde{\Psi}_m^\pm(\varphi, z), \quad (14)$$

where the "plus" sign corresponds to $z \to +\infty$ and the "minus" sign should be taken for $z \to -\infty$. Here $t_m^\pm$ is the partial transmission amplitude to the mode $\tilde{\Psi}_m^\pm(\varphi, z)$. As follows from Eq. (8), the amplitude is given by

$$t_m^\pm = \frac{i}{\sqrt{2\pi r k_m}} \sum_{j=1}^{N} \tilde{\xi}_j e^{\mp ik_m z_j - im\varphi_j}, \quad (15)$$

where $\tilde{\xi}_j = \xi_j m_w/\hbar^2$.

Denote the reflection coefficient to the wire $\mathbb{R}_j^+$ by $R_{11} = |S_1|^2$ and the transmission coefficient by $T_{j1} = |S_j|^2$. The partial transmission coefficient $T_m^\pm$ to the propagating mode $\tilde{\Psi}_m^\pm$ is defined by $T_m^\pm = (k_m/k)|t_m^\pm|^2$. We stress that the relation

$$R_{11} + \sum_{j=2}^{N} T_{j1} + \sum_{m=M^-}^{M^+} (T_m^+ + T_m^-) = 1 \quad (16)$$

is valid for an arbitrary energy E that is the manifestation of the current conservation law for our system.

Substituting Eq. (8) into Eq. (7), we get a system of $2N$ linear equations for S_j and ξ_j,

$$\begin{cases} \sum_{l=1}^{N} Q_{jl} \xi_l = B_{jj} \xi_j - \frac{ik\hbar^2 A_{jj}}{2m_w} (S_j - \delta_{j1}) \\ S_j + \delta_{j1} = A_{jj}^* \xi_j - \frac{ik\hbar^2 C_{jj}}{2m_w} (S_j - \delta_{j1}). \end{cases} \quad (17)$$

For convenience, we introduce the dimensionless elements of the Q-matrix,

$$\tilde{Q}_{ij}(E) = (\hbar^2/m_w)(Q_{ij}(E) - B_{ij}).$$

System (17) may be decomposed to a system of N equations for ξ_l,

$$\sum_{l=1}^{N} \left[\tilde{Q}_{jl} - \frac{2k\lambda_j^A \delta_{jl}}{k\lambda_j^C + 4i} \right] \tilde{\xi}_l = -\frac{4k\sqrt{\lambda_1^A} e^{i\phi_1}}{k\lambda_1^C + 4i} \delta_{j1} \quad (18)$$

and a similar system for S_l,

$$\sum_{l=1}^{N} \frac{\sqrt{\lambda_1^A}(k\lambda_l^C + 4i) e^{i\phi_l}}{\sqrt{\lambda_l^A}(k\lambda_1^C - 4i) e^{i\phi_1}} \left[\tilde{Q}_{jl} - \frac{2k\lambda_j^A \delta_{jl}}{k\lambda_j^C + 4i} \right] S_l = \tilde{Q}_{j1} - \frac{2k\lambda_1^A \delta_{j1}}{k\lambda_1^C - 4i}. \quad (19)$$

The solutions of systems (18) and (19) may be represented in the form
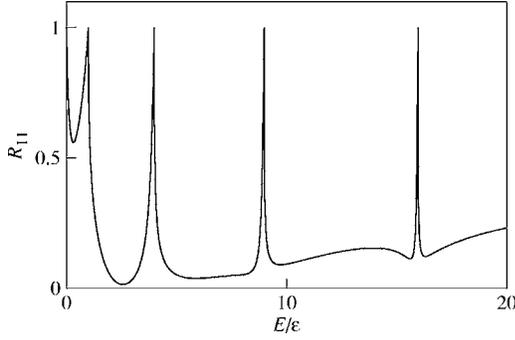
FIG. 2. Reflection coefficient as a function of the electron energy in the case of one wire attached to the cylinder at $\lambda_j^A = \lambda_j^B = \lambda_j^C = 0.4r$, $B = 0$.

$$\xi_n = \frac{\Delta_{\xi n}}{\Delta}, \qquad S_n = \frac{\Delta_{Sn}}{\Delta} \frac{\sqrt{\lambda_n^A}(k\lambda_1^C - 4i)e^{i\phi_1}}{\sqrt{\lambda_1^A}(k\lambda_n^C + 4i)e^{i\phi_n}}, \qquad (20)$$

where

$$\Delta = \det\left[\tilde{Q}_{jl} - \frac{2k\lambda_j^A \delta_{jl}}{k\lambda_j^C + 4i} \right], \qquad (21)$$

$$\Delta_{\xi n} = \det\left[\left(\tilde{Q}_{jl} - \frac{2k\lambda_j^A \delta_{jl}}{k\lambda_j^C + 4i} \right)(1 - \delta_{nl}) + \frac{4k\sqrt{\lambda_1^A}e^{i\phi_1}}{k\lambda_1^C + 4i}\delta_{j1}\delta_{nl} \right], \qquad (22)$$

and

$$\Delta_{Sn} = \det\left[\left(\tilde{Q}_{jl} - \frac{2k\lambda_j^A \delta_{jl}}{k\lambda_j^C + 4i} \right)(1 - \delta_{nl}) + \left(\tilde{Q}_{j1} - \frac{2k\lambda_1^A \delta_{j1}}{k\lambda_1^C - 4i} \right)\delta_{nl} \right]. \qquad (23)$$

III. RESULTS AND DISCUSSION

Let us consider in detail the case of one wire attached to the cylinder. Using Eqs. (15) and (20), we obtain

$$T_m^\pm = \frac{8k\lambda_1^A}{\pi r k_m |2k\lambda_1^A - (k\lambda_1^C + 4i)\tilde{Q}_{11}|^2}. \qquad (24)$$

Note that $T_m^+ = T_m^-$ for any energy E, i.e., the scattering is isotropic in the z direction. Reflection amplitude $r_{11} \equiv S_1$ may be obtained from Eq. (19),

$$r_{11} = \frac{(k\lambda_1^C - 4i)\tilde{Q}_{11} - 2k\lambda_1^A}{(k\lambda_1^C + 4i)\tilde{Q}_{11} - 2k\lambda_1^A}. \qquad (25)$$

The reflection coefficient $R_{11} = |r_{11}|^2$ as a function of the electron energy E is represented in Fig. 2. Hereafter we use $\varepsilon = \hbar^2/(2m_c r^2)$ for the unit of energy and suppose $m_w = m_c$. The figure shows that the dependence of reflection coefficient on E contains a series of sharp peaks at the points E_m. To study the behavior of the reflection coefficient in a vicinity of the eigenvalues E_m we consider the asymptotics of $\tilde{Q}_{jl}(E)$ near these points:
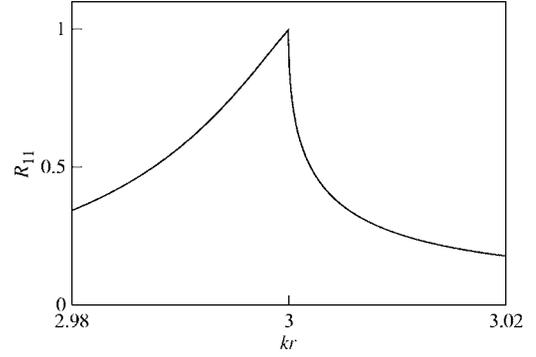
FIG. 3. Reflection coefficient as a function of the dimensionless parameter kr. All parameters are the same as in Fig. 2.

$$\tilde{Q}_{jl}(E) \simeq \frac{\alpha_{jl}^{(m)}}{k_m} + \beta_{jl}^{(m)} + O(k_m), \quad \text{as } k_m \to 0, \qquad (26)$$

where

$$\alpha_{jl}^{(m)} = i\sum_{m'} \Psi_{m'}(\varphi_j)\Psi_{m'}^*(\varphi_l) \qquad (27)$$

and m' are indices for which $E_{m'} = E_m$. If the magnetic flux Φ/Φ_0 is integer or half integer then the eigenvalues E_m are double degenerated and the sum in Eq. (27) contains two terms; otherwise it contains one term only.

As follows from Eq. (26), the denominator in Eq. (24) has a root singularity at $E = E_m$ while the numerator remains finite. Therefore all transmission coefficients $T_{m'}^\pm$ vanish and the reflection coefficient R_{11} reaches a unity. The reflection coefficient has a kink in a vicinity of each point E_m stipulated by the root singularity of the Green function on the cylinder. Using Eqs. (25) and (26), we obtain the following asymptotics for $R_{11}(k)$ near $\kappa_m = \sqrt{2m_w E_m}/\hbar$:

$$R_{11}(k) = \begin{cases} 1 - a_1(\kappa_m - k) + o(k_m^2), & \text{as } k \to \kappa_m - 0 \\ 1 - a_2\sqrt{k^2 - \kappa_m^2} + o(k_m), & \text{as } k \to \kappa_m + 0, \end{cases}$$

where a_1 and a_2 are positive numbers. The form of the reflection coefficient in a vicinity of the point E_3 is shown in Fig. 3.

The magnetic field splits double degenerated energy levels of the operator H_φ and peaks on the plot $R_{11}(kr)$ transform into doublets (Fig. 4). If the magnetic flux Φ/Φ_0 is half integer then the levels E_m are double degenerated and the peaks are singlet as for the case of integer flux, although their positions are shifted.

The reflection coefficient as a function of the magnetic field is shown in Fig. 5. Peaks on the plot correspond to the coincidence of the electron energy with the values E_m. Note that the function $R_{11}(\Phi)$ is periodic with a period Φ_0 that causes the Aharonov-Bohm oscillations in the transport. If the value of kr is integer or half integer then there is only one peak of $R_{11}(\Phi)$ on the period, otherwise there are two peaks on each cycle.

Let us turn to the case of two wires attached to the cylinder. Using Eq. (20), we obtain
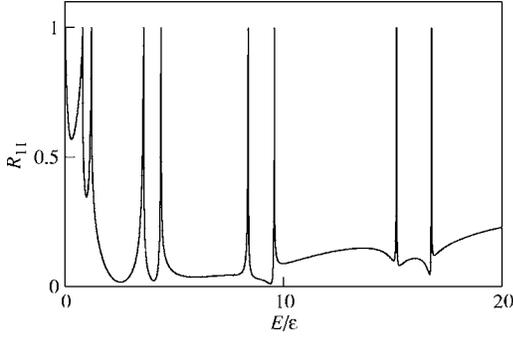
FIG. 4. Reflection coefficient at $\Phi/\Phi_0=0.1$. Other parameters are the same as in Fig. 2.

$$t_{21} = \frac{16ik\sqrt{\lambda_1^A \lambda_2^A} e^{i(\phi_1-\phi_2)}\widetilde{Q}_{21}}{(k\lambda_1^C + 4i)(k\lambda_2^C + 4i)\Delta}, \tag{28}$$

where

$$\Delta = \det \widetilde{Q} - \frac{2k\lambda_1^A}{k\lambda_1^C + 4i}\widetilde{Q}_{22} - \frac{2k\lambda_2^A}{k\lambda_2^C + 4i}\widetilde{Q}_{11}$$
$$+ \frac{4k^2\lambda_1^A\lambda_2^A}{(k\lambda_1^C + 4i)(k\lambda_2^C + 4i)}. \tag{29}$$

The transmissions coefficient $T_{21}=|t_{21}|^2$ as a function of the electron energy is shown in Fig. 6. The figure corresponds to the case when the contacts are placed on different generatrices ($\varphi_1 \neq \varphi_2$) and shifted along the axis of the cylinder ($z_1 \neq z_2$) in the zero magnetic field. One can see a series of zeros at $E=E_m$. Transmission coefficient has a peak in the neighborhood of each zero. The behavior of the transmission amplitude in a vicinity of the eigenvalues E_m depends strongly on contact position and applied magnetic field. If the points $\mathbf{q}_j$ are placed on the cylinder in a random manner, then the transmission coefficient vanishes at the double-degenerated values E_m. The denominator in Eq. (28) has a pole at $E=E_m$ while the numerator has a root singularity only. Hence the transmission coefficient vanishes in these points.

Let us consider in detail the form of the transmission coefficient in the vicinity of E_m. Using the asymptotic expres-

sion (26) for $\widetilde{Q}_{ij}(E)$, we obtain the following representation for $t_{21}(k)$:

$$t_{21}(k) \simeq c_m \frac{k_m}{f_m + k_m}, \tag{30}$$

as $E \to E_m$. Here c_m is a normalization factor and

$$f_m = \frac{\det \alpha^{(m)}}{\gamma_m} \tag{31}$$

is a complex number with

$$\gamma_m = \alpha_{11}^{(m)}\left(\beta_{22} - \frac{2\kappa_m\lambda_2^A}{(\kappa_m\lambda_2^C)^2 + 16}\right) + \alpha_{22}^{(m)}\left(\beta_{11} - \frac{2\kappa_m\lambda_1^A}{(\kappa_m\lambda_1^C)^2 + 16}\right)$$
$$- \alpha_{12}^{(m)}\beta_{21} - \alpha_{21}^{(m)}\beta_{12}.$$

One can see that the behavior of transmission coefficient in the vicinity of E_m is determined by the value f_m. Two curves for different positions of the contacts corresponding to different f_m are represented in Fig. 7. If $f_m \to 0$, then the transmission coefficient has a peak in a vicinity of the zero $k=\kappa_p$. The distance between the peak and the zero decreases with decreasing of $|f_m|$ while the peak value remains finite. The form of the graph in this region (dashed line in Fig. 7) resembles the form of the Fano resonance, but it is significant that the Fano curve is smooth in contrast to function (30). If $f_m=0$ then the peak and the zero of transmission coincide and cancel each other (solid line in Fig. 7). We note that f_m equals zero only if $\det \alpha^{(m)}=0$ as it follows from Eq.

FIG. 6. Transmission coefficient T_{21} as a function of the electron energy at $\varphi_1-\varphi_2=0.08\pi$, $z_1-z_2=0.2r$, and $\lambda_j^A=\lambda_j^B=\lambda_j^C=0.4r$.

FIG. 5. Reflection coefficient as a function of the magnetic field. Solid line: $k=4/r$; dashed line: $k=4.2/r$.
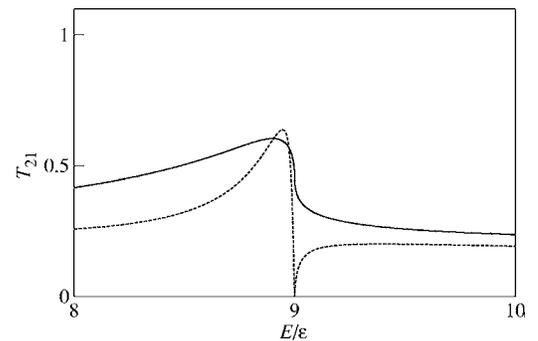
FIG. 7. Transmission coefficient T_{21} at $B=0$, $z_1-z_2=0.1r$, $\lambda_j^A=\lambda_j^B=\lambda_j^C=0.4r$. Solid line: $\varphi_1-\varphi_2=0$; dashed line: $\varphi_1-\varphi_2=0.08\pi$.
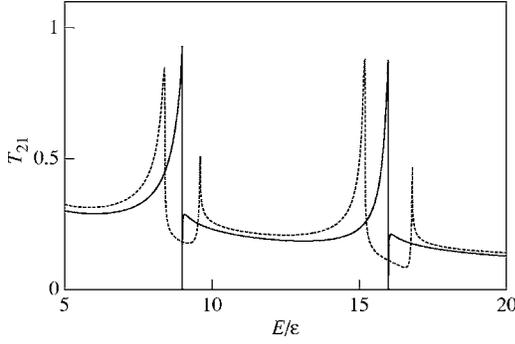
FIG. 8. Transmission coefficient T_{21} at $\lambda_j^A = \lambda_j^B = \lambda_j^C = 0.4r$, $z_1 - z_2 = 0.05r$, $\varphi_1 - \varphi_2 = 0.05\pi$. Solid line: $B = 0$; dashed line: $\Phi/\Phi_0 = 0.1$.

FIG. 9. Zero-temperature conductance G of the system as a function of the electron energy E at $\Phi/\Phi_0 = 0.1$. Other parameters are the same as in Fig. 8

(31). Therefore the form of the transmission coefficient in the vicinity of E_m is determined by the degree of degeneracy of E_m and by the symmetry of contact location. In particular det $\alpha^{(m)} = 0$ for all positions of contacts if the eigenvalue E_m is nondegenerated as it follows from Eq. (27). Therefore the zeros do not appear in a magnetic field with noninteger value of $2\Phi/\Phi_0$. The magnetic field splits double degenerated energy levels E_m and removes transmission zeros. The dependence $T_{21}(E)$ for the noninteger value of magnetic flux is represented in Fig. 8. One can see that the peaks on the plot $T_{21}(E)$ transform into doublets.

The value det α for integer $2\Phi/\Phi_0$ is given by

$$\det \alpha^{(m)} = -(\pi r)^{-2} \sin^2[(m + \Phi/\Phi_0)(\varphi_2 - \varphi_1)]. \quad (32)$$

If $\sin[(m + \Phi/\Phi_0)(\varphi_2 - \varphi_1)] = 0$ then the value f_m vanishes and the zero at the point E_m disappears. This phenomenon is similar to the collapse of the Fano resonance in the transmission through a quantum sphere.[3,4] The disappearance of the zeros is associated with the symmetry of the contact location. We note that all zeros disappear if the points $\mathbf{q}_1$ and $\mathbf{q}_2$ are placed on the same generatrix ($\varphi_1 = \varphi_2$) or on the opposite generatrices of the cylinder ($|\varphi_1 - \varphi_2| = \pi$). It is significant that the positions of all zeros are independent of the scattering lengths λ_j^A, λ_j^B, and λ_j^C.

In the case of $f_m = 0$ the transmission coefficient T_{21} may be represented near E_m in the form

$$T_{21}(k) \simeq |c_m|^2 |1 + g_m k_m|^2,$$

where c_m is a normalization factor and g_m is a complex number depending on the position of contacts and scattering lengths. The smoothness of the curve $T_{21}(E)$ at the point $E = E_m$ is determined by the number g_m. Indeed, the left-hand derivative is infinite in this point if Im $g_m \neq 0$ and the right-hand derivative is infinite for Re $g_m \neq 0$. If the one-sided derivatives are different, then the transmission coefficient has a kink at the point E_m. The solid line in Fig. 7 corresponds to the case of infinite derivatives.

According to the Landauer-Büttiker formalism the ballistic conductance G of the device at the zero temperature is determined by transmission probabilities $T_{21}^\uparrow$ and $T_{21}^\downarrow$,
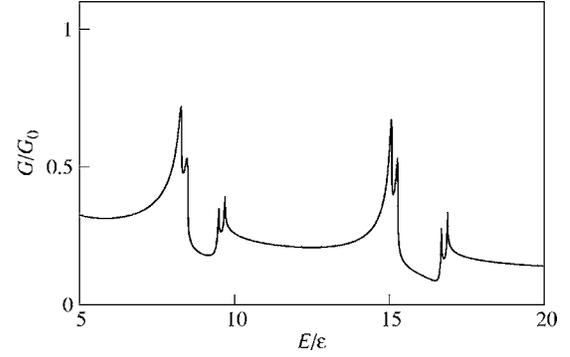
$$G = G_0(T_{21}^\uparrow + T_{21}^\downarrow), \quad (33)$$

where $G_0 = e^2/(2\pi\hbar)$ is the conductance quantum. The conductance as a function of the electron energy is shown in Fig. 9. The dependence of the transmission coefficient on electron spin orientation in the magnetic field results in additional splitting of conductance peaks (Fig. 9) and partial spin polarization of transmitted electrons. It should be mentioned that the spin splitting $g\mu_B B$ is independent of magnetic quantum number m while the splitting of the eigenvalues E_m is proportional to m, hence the peaks are not equidistant. It is essential that the spin polarization can be changed either by magnetic field or by electron energy. The complete polarization is possible for integer and half integer values of magnetic flux Φ/Φ_0.

The conductance oscillates as a function of energy with the period,

$$\Delta E \simeq \frac{\pi}{L}\frac{dE}{dk_m} = \frac{\pi h^2 k_m}{4m_c L}, \quad (34)$$

if the longitudinal distance $L = |z_1 - z_2|$ between the points $\mathbf{q}_1$ and $\mathbf{q}_2$ is much larger than the radius r (see Fig. 10). The oscillations are stipulated by the interference of electron waves on the cylinder. It should be noted that similar oscillations have been observed in a recent experiment[8] with carbon nanotubes. The geometry of the experiment differs from
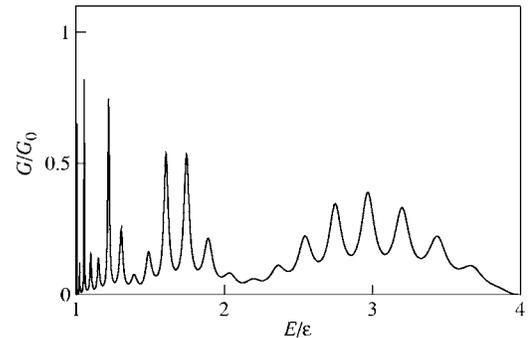
FIG. 10. Zero-temperature conductance G of the system as a function of the electron energy at $z_1 - z_2 = 40r$, $\varphi_1 = \varphi_2$, $\lambda_j^A = \lambda_j^B = \lambda_j^C = 0.4r$, and $B = 0$.

ours; in particular, contacts are not pointlike. But some results are valid for our system as well, in particular, the estimation for the period of oscillations carried out in Ref. 8 is in agreement with Eq. (34).

IV. CONCLUSION

Electron transport in a nanodevice consisting of a conductive cylinder with one-dimensional wires connected to its lateral surface is considered. The one-particle Hamiltonian of the system is obtained using linear boundary conditions at the points of contact. An explicit form for transmission and reflection coefficient as a function of electron energy is found by solving the Schrödinger equation. The general case of arbitrary number of wires and arbitrary disposition of contacts is considered. Two cases corresponding to a single wire and two wires attached to the cylinder surface are studied in detail. It is found that reflection peaks occur at energies coinciding with the discrete part E_m of the electron spectrum on the cylinder. The form of reflection peaks is discussed.

A similar analysis of the two-wire case shows that the transmission coefficient equals zero at energies E_m. We have found that asymmetric Fano-type resonances appear in a vicinity of the zeros. The zeros exist only if the number of magnetic-flux quanta through the cylinder is integer or half integer. They exist for all positions of contacts $\mathbf{q}_1$ and $\mathbf{q}_2$ except some specific points. It is shown that the zero at the point E_m disappears if the value det $\alpha^{(m)}$ defined by Eq. (32) vanishes. The behavior of the transmission coefficient in this case resembles the collapse of the Fano resonances discussed in earlier studies.[4,36]

The conductance of the device is investigated using Landauer-Buttiker formalism. The resonances in transmission coefficient lead to appearance of conductance oscillations. The magnetic field splits conductance peaks and causes spin polarization of transmitted electrons. The complete spin polarization is possible for integer and half integer values of the magnetic flux.

The results of the paper may be useful for the study of electron transport in single-wall carbon nanotubes and rolled GaAs/AlGaAs heterostructures. The experimental observation of the discussed effects should become possible involving leads thin enough, like the tip of the scanning tunnel microscope. The geometry of the device in the case of one wire resembles the geometry of experiments on scanned probe microscopy of carbon nanotubes.[32,33] Experimental setup using two tips on the same nanotube seems in principle feasible, although perhaps difficult to realize. In the case of multimode leads the interference of electron waves from different modes will most probably result in additional transmission peaks and minima. We stress that most of the obtained results reflect the intrinsic properties of electron motion on the cylinder. Therefore they are expected to remain valid qualitatively even in the case of realistic non-one-dimensional wires.

*Electronic address: pyataevma@math.mrsu.ru

[1] C. L. Foden, M. L. Leadbeater, and M. Pepper, Phys. Rev. B **52**, R8646 (1995).

[2] A. Kiselev, J. Math. Anal. Appl. **212**, 263 (1997).

[3] J. Brüning, V. A. Geyler, V. A. Margulis, and M. A. Pyataev, J. Phys. A **35**, 4239 (2002).

[4] V. A. Geyler, V. A. Margulis, and M. A. Pyataev, Zh. Eksp. Teor. Fiz. **124**, 851 (2003) [JETP **97**, 763 (2003)].

[5] V. A. Margulis and M. A. Pyataev, J. Phys.: Condens. Matter **16**, 4315 (2004).

[6] A. V. Chaplik, L. I. Magarill, and D. A. Romanov, Physica B **249-251**, 377 (1998).

[7] L. I. Magarill, D. A. Romanov, and A. V. Chaplik, Zh. Eksp. Teor. Fiz. **113**, 1411 (1998) [JETP **86**, 771 (1998)].

[8] J. Kong, E. Yenilmez, T. W. Tombler, W. Kim, H. Dai, R. B. Laughlin, L. Liu, C. S. Jayanthi, and S. Y. Wu, Phys. Rev. Lett. **87**, 106801 (2001).

[9] J. Kim, J. R. Kim, Jeong-O Lee, J. W. Park, H. M. So, N. Kim, K. Kang, K.-H. Yoo, and J.-J. Kim, Phys. Rev. Lett. **90**, 166403 (2003).

[10] B. Babič and C. Schönenberger, Phys. Rev. B **70**, 195408 (2004).

[11] B. Gao, A. Komnik, R. Egger, D. C. Glattli, and A. Bachtold, Phys. Rev. Lett. **92**, 216804 (2004).

[12] J. Appenzeller, J. Knoch, M. Radosavljevic, and Ph. Avouris, Phys. Rev. Lett. **92**, 226802 (2004).

[13] V. Ya. Prinz, V. A. Seleznev, A. K. Gutakovsky, A. V. Chehovskiy, V. V. Preobrazhenskii, M. A. Putyato and T. A. Gavrilova, Physica E (Amsterdam) **6**, 828 (2000).

[14] A. B. Vorob'ev, V. Ya. Prinz, Yu. S. Yukecheva, and A. I. Toropov, Photonics Spectra **23**, 171 (2004).

[15] M. B. Nardelli, Phys. Rev. B **60**, 7828 (1999).

[16] M. P. Anantram and T. R. Govindan, Phys. Rev. B **61**, 5020 (1999).

[17] H. J. Choi and J. Ihm, Solid State Commun. **111**, 385 (1999).

[18] S. Sanvito, Y.-K. Kwon, D. Tomanek, and C. J. Lambert, Phys. Rev. Lett. **84**, 1974 (2000).

[19] G. Fagas, G. Cuniberti, and K. Richter, Phys. Rev. B **63**, 045416 (2001).

[20] R. Gutierrez, G. Fagas, G. Cuniberti, F. Grossmann, R. Schmidt, and K. Richter, Phys. Rev. B **65**, 113410 (2002).

[21] S. Uryu, Phys. Rev. B **69**, 075402 (2004).

[22] O. V. Kibis, D. G. W. Parfitt, and M. E. Portnoi Phys. Rev. B **71**, 035411 (2005).

[23] T. Ando, Semicond. Sci. Technol. **15**, R13 (2000).

[24] E. G. Emberly and G. Kirczenow, Phys. Rev. B **62**, 10451 (2000).

[25] B. S. Pavlov, I. Yu. Popov, V. A. Geyler, and O. S. Pershenko, Europhys. Lett. **52**, 196 (2000).

[26] D. Csontos and H. Q. Xu, J. Phys.: Condens. Matter **14**, 12513 (2002).

[27] H. Q. Xu, Phys. Rev. B **66**, 165305 (2002).

[28] G. Cuniberti, J. Yi, and M. Porto, Appl. Phys. Lett. **81**, 850 (2002).

[29] D. Csontos and H. Q. Xu, Phys. Rev. B **67**, 235322 (2003).

[30] C. D. Spataru and P. Budau, J. Phys.: Condens. Matter **14**, 4995 (2002).

[31] L. F. Chibotaru, S. Compernolle, and A. Ceulemans Phys. Rev. B **68**, 125412 (2003).

[32] A. Bachtold, M. S. Fuhrer, S. Plyasunov, M. Forero, Erik H. Anderson, A. Zettl, and Paul L. McEuen, Phys. Rev. Lett. **84**, 6082 (2000).

[33] Y. Yaish, J.-Y. Park, S. Rosenblatt, V. Sazonova, M. Brink, and P. L. McEuen, Phys. Rev. Lett. **92** 046401 (2004).

[34] K. A. Dick, K. Deppert, M. W. Larsson, T. Mrtensson, W. Seifert, L. R. Wallenberg, and L. Samuelson, Nat. Mater. **3**, 380 (2004)

[35] C. S. Kim and A. M. Satanin, Zh. Eksp. Teor. Fiz. **115**, 211 (1999) [JETP **88**, 118 (1999)].

[36] C. S. Kim, A. M. Satanin, Y. S. Joe, and R. M. Cosby, Zh. Eksp. Teor. Fiz. **116**, 263 (1999) [JETP **89**, 144 (1999)].

[37] C. S. Kim and A. M. Satanin, Physica E (Amsterdam) **4**, 211 (1999).

[38] C. S. Kim, O. N. Roznova, A. M. Satanin, and V. B. Stenberg, Zh. Eksp. Teor. Fiz. **121**, 1157 (2002) [JETP **94**, 992 (2002)].

[39] P. Exner and P. Šeba, J. Math. Phys. **28**, 386 (1987).

[40] J. Brüning and V. A. Geyler, J. Math. Phys. **44**, 371 (2003).

[41] P. Exner, R. Gawlista, P. Seba, and M. Tater, Ann. Phys. (N.Y.) **252**, 133 (1996).

[42] V. A. Geiler, V. A. Margulis, and I. I. Chuchaev, Fiz. Tverd. Tela (Leningrad) **37**, 837 (1995) [Phys. Solid State **37**, 455 (1995)].